ELSEVIER

Ceramics International 25 (1999) 197–200

CERAMICS INTERNATIONAL

Short communication

Electrical properties of lithium zirconium phosphate ceramics prepared from $ZrLi_XH_{2-X}P_2O_8{\cdot}nH_2O$

Susumu Nakayama [a,*], Katsuhiko Itoh [b], Shinichi Kakita [b], Toshihisa Suzuki [b], Masatomi Sakamoto [c]

[a] *Department of Applied Chemistry and Biotechnology, Niihama National College of Technology, 7-1, Yagumo-cho, Niihama-shi 792-8580, Japan*
[b] *Development Division, Daiichi Kigenso Kagaku Kogyo Co., Ltd., 4-4-14, Kouraibashi, Chuo-ku, Osaka-shi 541-0043, Japan*
[c] *Department of Material and Biological Chemistry, Faculty of Science, Yamagata University, 1-4-12, Kojirakawa-mati, Yamagata-shi 990-8560, Japan*

Received 19 October 1997; accepted 8 January 1998

Abstract

Lithium zirconium phosphates with various compositions were prepared by sintering $ZrLi_XH_{2-X}P_2O_8{\cdot}nH_2O$ with $0.5 \leqq X \leqq 2.0$ at 1000°C, and microstructure, crystal phases and electrical properties were examined on the sintered products. Lithium ion conductive $Li_2ZrP_2O_8$ and insulative ZrP_2O_7 were the predominant phases in the sintered products with $X \geqq 1.0$ and $X \leqq 0.8$, respectively. Electrical properties varied with changes in the ratio of the phases present and the microstructure forms which depend on the lithium ion content. The highest conductivity (6.6×10^{-4} S cm^{-1}) at 200°C was achieved for the sintered product with $X = 1.6$.

Keywords: Lithium zirconium phosphate; Lithium ionic conductor; Ceramic electrolyte

1. Introduction

Studies of the superionic conductors have been widely undertaken for the development of solid state batteries and chemical sensors [1,2]. Sintered products in the system $ZrM_XH_{2-X}P_2O_3{\cdot}nH_2O$, where M = H, Li, Na, K, Rb, Cs or Ag and $X = 1.0$ or 2.0, is one group of the well-studied materials [3–5]. A product of $ZrLi_2P_2O_8{\cdot}nH_2O$ sintered at 1000°C for 3 h was found to show the highest ionic conductivity (1.5×10^{-4} S cm^{-1} at 200°C) among these materials [3]. However, the electrical properties of the family of lithium zirconium phosphate have not been systematically investigated.

In this work, lithium zirconium phosphates with various composition (abbreviated as ZrP–LiX) were prepared by sintering the crystalline powders of $ZrLi_XH_{2-X}P_2O_8{\cdot}nH_2O$, where X is 0.5, 0.8, 1.0, 1.5, 1.6, 1.7 or 2.0. Based on the measured electrical properties, the effect of lithium content on the electrical properties were studied.

2. Experimental

α-Zirconium bis(monohydrogen phosphate) monohydrate, α-$ZrH_2P_2O_8H_2O$, was prepared by the reflux of amorphous zirconium phosphate with an excess of phosphoric acid for 100 h. The product was washed with distilled and deionized water, and dried at 60°C. Various compositions of crystalline lithium–substituted zirconium hydrogen phosphates, $ZrLi_XH_{2-X}P_2O_8{\cdot}nH_2O$, were obtained with dropwise addition of a lithium hydroxide solution to a suspension of α-$ZrH_2P_2O_8{\cdot}H_2O$ in distilled and deionized water under stirring. All of the products were washed with purified water and then dried at 60°C. The compositions of $ZrLi_XH_{2-X}P_2O_8{\cdot}nH_2O$ prepared were determined by the elemental analysis (Table 1). It was confirmed that all $ZrLi_XH_{2-X}P_2O_8{\cdot}nH_2O$ retained a layered structure observed in α-$ZrH_2P_2O_8{\cdot}H_2O$ by the standard X-ray diffraction technique (XRD). After these products were pulverized using a ball-mill, the powder obtained was pressed at 100 MPa and sintered at 1000°C for 3 h. The prepared discs were 9 mm in diameter and 3 mm thickness. Next, platinum electrodes were applied to opposite faces by fired platinum paste at 900°C. Measurements

* Corresponding author.

0272-8842/99/$—see front matter
PII: S0272-8842(98)00008-X

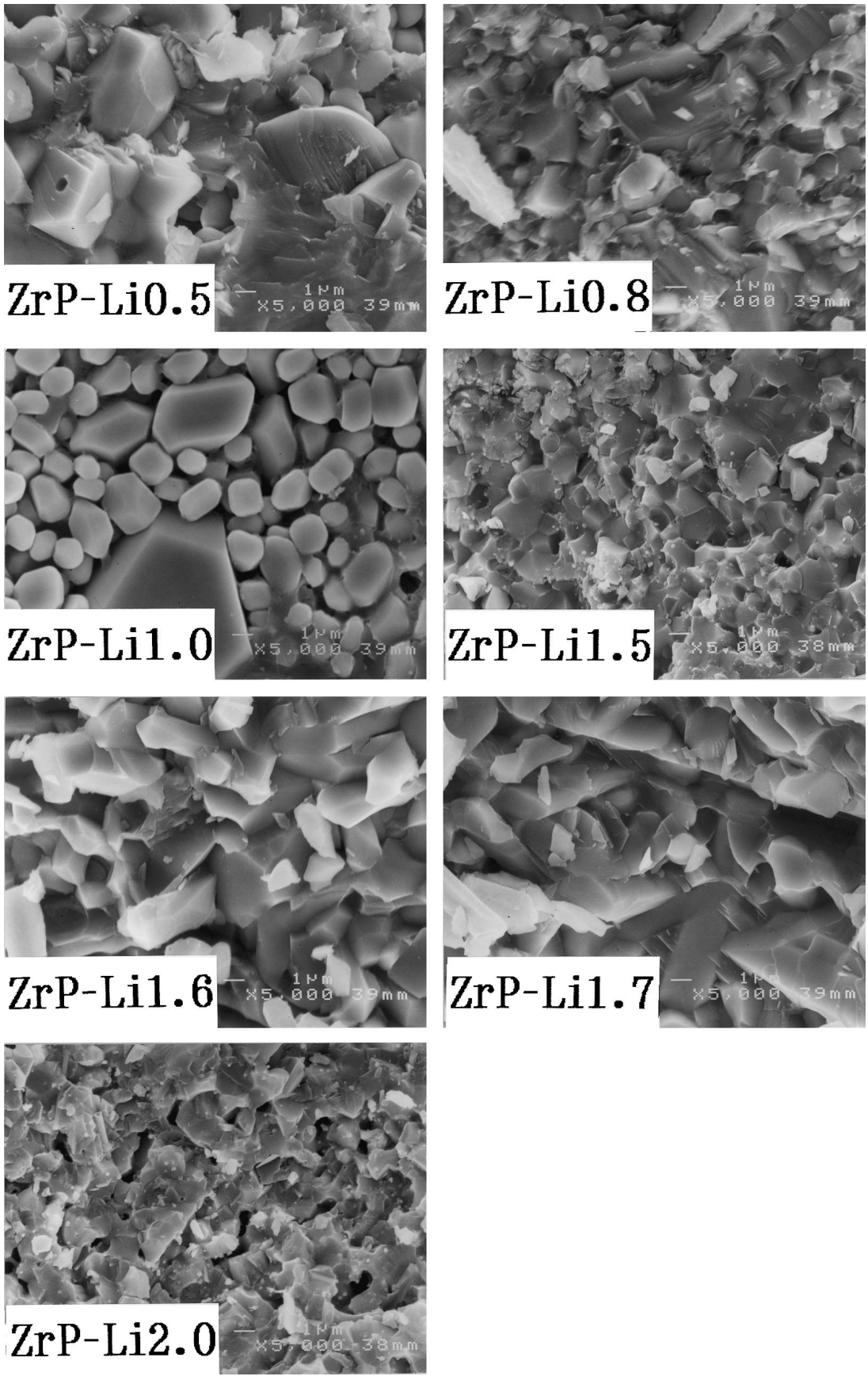

Fig. 1. Scanning electron micrographs of the sintered products of $ZrLixH_{2-x}P_2O_8 \cdot nH_2O$ (bar + 1 μm).

Table 1
Parameters of electrical properties

Starting material	E ($kJ \cdot mol^{-1}$)	Conductivity ($S \cdot cm^{-1}$)		
		200°C	300°C	400°C
$ZrLi_{0.5}H_{1.5}(PO_4)_2 \cdot H_2O$	88	1.75×10^{-7}	7.52×10^{-6}	9.71×10^{-5}
$ZrLi_{0.8}H_{1.2}(PO_4)_2 \cdot 2H_2O$	93	1.09×10^{-6}	6.03×10^{-5}	6.33×10^{-4}
$ZrLi_{1.0}H_{1.0}(PO_4)_2 \cdot 5H_2O$	102[a] (64[b])	2.71×10^{-6}	2.27×10^{-4}	2.38×10^{-3}
$ZrLi_{1.5}H_{0.5}(PO_4)_2 \cdot 2H_2O$	69[c] (50[d])	3.94×10^{-4}	4.42×10^{-3}	1.44×10^{-2}
$ZrLi_{1.6}H_{0.4}(PO_4)_2 \cdot 2H_2O$	68[c] (41[d])	6.62×10^{-4}	7.35×10^{-3}	2.00×10^{-2}
$ZrLi_{1.7}H_{0.3}(PO_4)_2 \cdot 6H_2O$	64[c] (48[d])	4.98×10^{-4}	4.33×10^{-3}	1.39×10^{-3}
$ZrLi_{2.0}(PO_4)_2 \cdot 2H_2O$	62[c] (50[d])	1.31×10^{-4}	1.31×10^{-3}	4.33×10^{-3}

[a] < 350°C; [b] > 350°C; [c] < 250°C, [d] > 250°C.

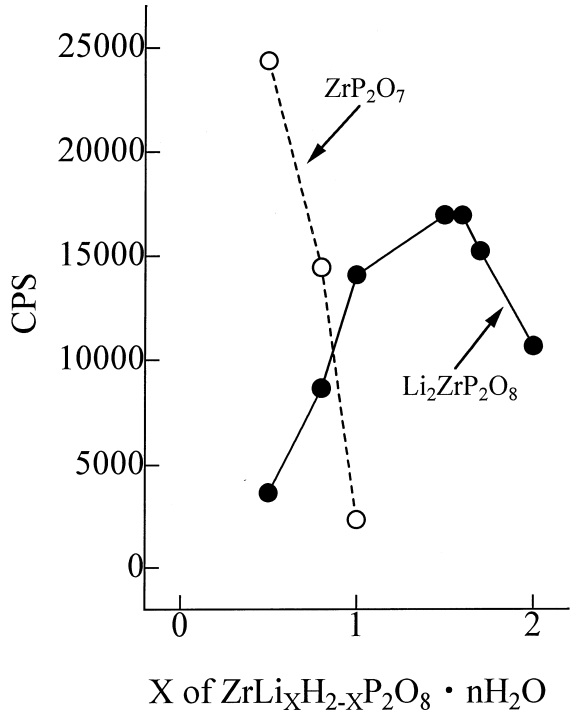

Fig. 2. XRD peak intensities of $Li_2ZrP_2O_8$ (peak assigned to that of $d = 4.42$ in JCPDS no. 38-278) and ZrP_2O_8 (peak assigned to that of $d = 4.12$ (hkl = 600) in JCPDS no. 24-1490) present in the sintered products of $ZrLi_xH_{2-x}P_2O_8 \cdot nH_2O$.

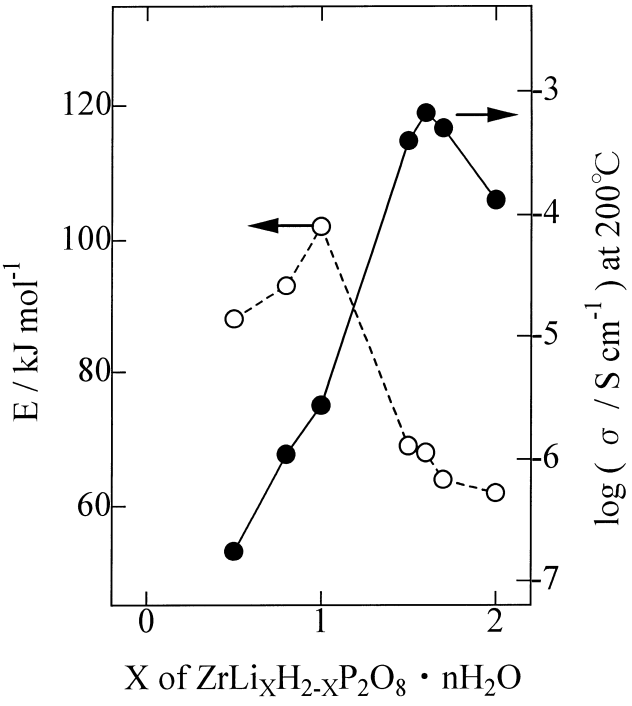

Fig. 3. Relationship between the substituted lithium amount and electrical properties for the sintered products of $ZrLi_xH_{2-x}P_2O_8 \cdot nH_2O$.

were carried out using an impedancemeter, YHP 4192A, in the frequency range of 100 Hz to 10 MHz. The crystalline phases were identified at room temperature by XRD. The microstructure of fractured face was examined using scanning electron microscopy (SEM).

3. Results and discussion

Fig. 1 shows the microstructure of ZrP–Li*X*, the sintered products of $ZrLi_XH_{2-X}P_2O_8 \cdot nH_2O$. In all cases, the layered morphologies observed in $ZrLi_XH_{2-X}P_2O_8 \cdot nH_2O$ were disappeared after sintering. The particle sizes are 5 μm or more in diameter for ZrP–Li0.5, ZrP–Li0.8, ZrP–Li1.6 and ZrP–Li1.7, and 2-4 μm diameter for ZrP–Li1.5 and ZrP–Li2.0. The microstructure of ZrP–Li1.0 is very different from those of others. It consists of round particles of 2-6 μm diameter and the densification seems to have not proceeded well.

Fig. 2 shows the relationship between the *X*-values and the XRD peak intensities of $Li_2ZrP_2O_8$ and ZrP_2O_7 present in the ZrP–Li*X*. For ZrP–Li1.5, ZrP–Li1.6, ZrP–Li1.7 and ZrP–Li2.0, the main peaks were assigned to $Li_2ZrP_2O_8$ and other minor peaks were assigned to $LiZr_2P_3O_{12}$ and Li_3PO_4. For ZrP–Li1.0, peaks assignable to ZrP_2O_7 were observed, though the peaks assigned to $Li_2ZrP_2O_8$ are still predominant. On the other hand, the peaks of ZrP_2O_7 were predominant for ZrP–Li0.5 and ZrP–Li0.8, though those of $Li_2ZrP_2O_8$

were also observed. As a result, it may be concluded that the main phase is $Li_2ZrP_2O_8$ for the ZrP–Li1.0, ZrP–Li1.5, ZrP–Li1.6, ZrP–Li1.7 and ZrP–Li2.0, and ZrP_2O_7 for ZrP–Li0.5 and ZrP–Li0.8.

In order to determine the electrical conductivity, complex-plane impedance analysis was applied at various temperatures in the range of 100 to 500°C. The results fall on an arc which passes through the origin of the complex-plane impedance plot (i.e., Cole–Cole plot: x-axis, real; y-axis, imaginary part). From these observed results, the total conductivity (the sum of the grain boundary and the grain) was determined by an extrapolation to zero reactance of the complex impedance plot in the low-frequency region. The conductivity data were parameterized by the Arrhenius equation

$$\sigma T = \sigma_0 \exp(-E/kT)$$

whereσ, σ_0 E, k and T stand for the conductivity, the pre-exponential factor, the activation energy, the Boltzmann constant and the absolute temperature, respectively. The electrical properties obtained are summarized in Table 1, and the relationships between the X-values of ZrP–LiX and the activation energies at 200°C or conductivities are shown in Fig. 3. The conductivity increased with increasing X-value from 0.5 to 1.6 and then decreased with increasing X-value from 1.6 to 2.0. Here, it should be noted that the conductivity (1.3×10^{-4} S cm^{-1}) of ZrP–Li2.0 at 200°C is in good agreement with that (1.5×10^{-4} S cm^{-1}) of a product of $ZrLi_2P_2O_8{\cdot}nH_2O$ sintered at 1000°C for 3 h reported by Sadaoka and Sakai [3]. The highest conductivity at 200°C is 6.6×10^{-4} S cm^{-1} for ZrP–Li1.6. The ZrP–LiXs are classified into two groups in terms of the activation energies. One is the group of ZrP–LiX with $1.5 \leqq X \leqq 2.0$. The activation energies of the this group are in the range of 62 to 69 kJ mol^{-1}, which are lower than those (88 to 102 kJ mol^{-1}) of another group of ZrP–LiX with $X \leqq 1.0$. Low activation energies and high conductivities of former group may be due to the formation of a large amount of $Li_2ZrP_2O_8$ which is well known as a crystal phase exhibiting high conduction of lithium ions (3.2×10^{-4} S cm^{-1} at 200°C) [6]. On the other hand, high activation energies and low conductivities for ZrP–Li0.5 and ZrP–Li0.8 may be due to the formation of a large amount of ZrP_2O_7 known as a insulative material (3.6×10^{-7} S cm^{-1} at 300°C) [7]. The ZrP–Li1.0 composition exhibits high activation energy and low conductivity, despite that $Li_2ZrP_2O_8$ is a predominant phase. This may be explained by the following reasons: first, ZrP_2O_7 is partially formed, as can be seen from Fig. 2; second, the sintering of ZrP–Li1.0 is poorer, compared with those of other samples (Fig. 1).

Thus, the conductivity of the sintered products of $ZrLi_XH_{2-X}P_2O_8{\cdot}nH_2O$ was found to be affected by the ratio of the phases present and the microstructure forms which depend on the lithium ion content.

Acknowledgements

The authors thank Mr. R. Yajima, a former managing director of Shinagawa Refractories Co., Ltd., for his helpful advice.

References

[1] H. Aono, E. Sugimoto, Y. Sadaoka, N. Imanaka, G. Adachi, The electrical properties of ceramic electrolytes for $LiM_XTi_{2-X}(PO_4)_3 + yLi_2O$, M = Ge, Sn, Hf, and Zr system, J. Electrochem. Soc. 140 (1993) 1827–1933.

[2] S. Nakayama, Y. Sadaoka, Preparation of an $Na_3Zr_2Si_2PO_{12}$–sodium aluminosilicate composite and its application as a solid-state electrochemical CO_2 gas sensor, J. Mater. Chem. 4 (1994) 663–668.

[3] Y. Sadaoka, Y. Sakai, Ionic conductivity of burnt $Zr(LiPO_4)_2{\cdot}xH_2O$, J. Mater. Sci. Lett. 5 (1986) 731–732.

[4] Y. Sadaoka, M. Matsuguchi, Y. Sakai, S. Mitsui, M. Toita, K. Hatanaka, Effects of firing temperature on morphology and crystal structure of zirconium bis(monohydrogen phosphate) and its alkali salts, J. Mater. Sci. 24 (1989) 432–438.

[5] Y. Sadaoka, Y. Sakai, M. Matsuguchi, Ionic conductivity and crystal structure of fired crystalline zirconium phosphate completely and half exchanged with some monovalent cations, J. Mater. Sci. 24 (1989) 2081–2092.

[6] M. de L. Chavez, P. Quintana, A.R. West, New Li^+ ion conductors, $Li_{2-4X}Zr_{1+X}(PO_4)_2$, Mat. Res. Bull. 21 (1986) 1411–1416.

[7] R. Saks, Y. Avigol, E. Banks, New solid electrolytes based on cubic ZrP_2O_7, J. Electrochem. Soc. 129 (1982) 726–729.